

Synthesis of three-component high nuclearity cluster complexes with ruthenium carbido carbonyl clusters as a building block

Takayuki Nakajima ^{a,*}, Hiromi Konomoto ^b, Haruo Ogawa ^b, Yasuo Wakatsuki ^c

^a Department of Applied Chemistry, School of Science and Engineering, Waseda University, Okubo 3-4-1 Shinjuku-ku, Tokyo 169-8555, Japan

^b Department of Chemistry, Tokyo Gakugei University, Koganei-shi, Tokyo 184-8501, Japan

^c Department of Chemistry, College of Humanities and Sciences, Nihon University, Sakurajosui 3-25-40, Setagaya-ku, Tokyo 156-8550, Japan

Received 8 June 2007; received in revised form 17 July 2007; accepted 24 July 2007

Available online 8 August 2007

Abstract

Treatment of AgNO₃ with the Rh–Ru and Cu–Ru hetero bimetallic clusters, [PPN][RhRu₅C(CO)₁₄(cod)] and [PPh₄]₂[CuRu₆C(CO)₁₆Cl], afforded novel three-component complexes having one silver-, and two silver-bridges between respective cluster units, [PPN]{Ag[RhRu₅C(CO)₁₄(cod)]₂} and [PPh₄]₂{Ag₂[CuRu₆C(CO)₁₆Cl]₂}, respectively. Reaction of the ruthenium–copper cluster [PPh₄]₂{Cu₄[Ru₆C(CO)₁₆]₂Cl₂} (**6**) with Pd₂(dba)₃ · CHCl₃ gave another three-component cluster [PPh₄]₂{Cu₄Pd₂[Ru₆C(CO)₁₆]₂Cl₂} by incorporation of two palladium atoms. However, a similar reaction of **6** with Pt(dba)₂ gave only a two-component cluster complex, [PPh₄]₂{Pt₂[Ru₆C(CO)₁₅]₂}, while the reaction of silver analog [PPN]₂{Ag₄[Ru₆C(CO)₁₆]₂Cl₂} with Pd₂(dba)₃ · CHCl₃ resulted in the formation of known ruthenium–palladium cluster [PPN]₂{Pd₄[Ru₆C(CO)₁₆]₂}. Treatment of **6** with [RhCl(CO)₂]₂ gave two two-component clusters, [PPh₄][RhRu₅C(CO)₁₆] and [PPh₄]₂{Cu₇[Ru₆C(CO)₁₅]₂Cl₃}. All the new mixed-metal high nuclearity clusters have been characterized by single crystal X-ray analyses.

© 2007 Elsevier B.V. All rights reserved.

Keywords: Three-component cluster; High-nuclearity mixed-metal cluster; Ruthenium carbido carbonyl cluster

1. Introduction

High-nuclearity mixed-metal cluster complexes have attracted considerable interest because of their diverse applications [1,2]. One example, which may be useful as nano-materials and heterogeneous catalysts, is their application as precursors for tiny metal alloy dispersions with discrete metal atom composition. For this purpose, mixed-metal clusters based on metal carbonyls and their olefin-substituted derivatives are particularly useful, since the transformation of such cluster molecules to metal alloy particles is generally an easy process. To date, a large number of two-component mixed-metal carbonyl clusters have been reported. One of the most straightforward routes to them is the ionic coupling reaction, or redox condensation, between a carbonyl cluster anion and a cationic metal spe-

cies [1,3–28]. For example, we previously applied this type of reaction to a combination of anionic ruthenium carbido carbonyl clusters with a cationic palladium mononuclear complex to give neutral high-nuclearity Pd–Ru mixed-metal complexes, where eight Pd atoms segregated between two five-nuclear Ru–cluster units [29].

If a two-component cluster prepared in this way still carries negative charge and that charge is not too delocalized over the whole cluster moiety, it should potentially have chance to react further with a third cationic metal species to give three-component mixed-metal clusters of higher nuclearity. Since examples of three-component mixed-metal clusters are quite limited [30–35], we decided to synthesize such heterometallic carbonyl clusters mainly by adopting the redox condensation reactions using a ruthenium carbido carbonyl cluster as the initial anionic block. In this report, successful preparation of high nuclearity cluster complexes comprising of three different transition metals (Ag, Rh, Ru), (Ag, Cu, Ru), and (Cu, Ru, Pd) is

* Corresponding author.

E-mail address: t.nakajima@cc.nara-wu.ac (T. Nakajima).

described. In addition, several new two-component mixed-metal carbonyl clusters, which resulted from our effort of preparing three-component systems, are also reported.

2. Results and discussions

2.1. Synthesis of $\{Ag[RhRu_5C(CO)_{14}(cod)]_2\}^-$ cluster complex

We previously found that a 1D polymer complex $[PPN][AgRu_6C(CO)_{16}]_\infty$ ($PPN = N(PPh_3)_2^+$) is formed simply by mixing $[PPN]_2[Ru_6C(CO)_{16}]$ and $AgNO_3$ in equimolar amounts [36]. In order to synthesize Ag–Rh–Ru thrimetallic cluster by applying such reactions, we used the Rh–Ru bimetallic cluster $[PPN][RhRu_5C(CO)_{14}(cod)]$ (**1**, $cod = 1,5$ -cyclooctadiene) [37,38]. Complex **1** reacted smoothly with 0.5 equivalent $AgNO_3$ in THF at room temperature and the process was conveniently monitored by sampling a small portion and measuring its IR signals. After 12 h, the reaction mixture was worked up on a column chromatography to give dark-red crystals of the composition $[PPN]\{Ag[RhRu_5C(CO)_{14}(cod)]_2\}^-$ (**2**) in 83% yield. The solid state structure of **2** has been deter-

mined by single-crystal X-ray diffraction as shown in Fig. 1, which shows that the silver atom bridges two mixed-metal cluster units in a manner similar to that observed in the 1D polymer $[PPN][AgRu_6C(CO)_{16}]_\infty$. When one equivalent of $AgNO_3$ was used, however, the sandwich type cluster **2** was again obtained. There is a crystallographic center of symmetry at the silver atom, which has a distorted tetrahedral bonding, the dihedral angle $Ag-Ru(12)-Ru(13)/Ag-Ru(12)^*-Ru(13)^*$ being 47.5° . The $Ag-Ru(12)$ and $Ag-Ru(13)$ bond lengths are 2.9118(2) and 2.9293(4) Å, respectively (Table 1). The $Ru(12)-Ru(13)$ edge bridged by the silver atom is 3.09747(5) Å long, which is significantly longer than the other $Ru-Ru$ bonds (average 2.861 Å). A similar trend is observed in the 1D polymer $[PPN][AgRu_6C(CO)_{16}]_\infty$, where the corresponding distance is 3.046(1) Å [36]. The 1H NMR spectrum of **2** shows three broad singlets for the two cyclooctadiene ligands which are bonded solely to each rhodium. The variable temperature 1H NMR spectrum at $-60^\circ C$ showed sharp but complex multiplets, indicating that the cod ligand is fluxional at room temperature, probably rotating in the same coordination site of Rh.

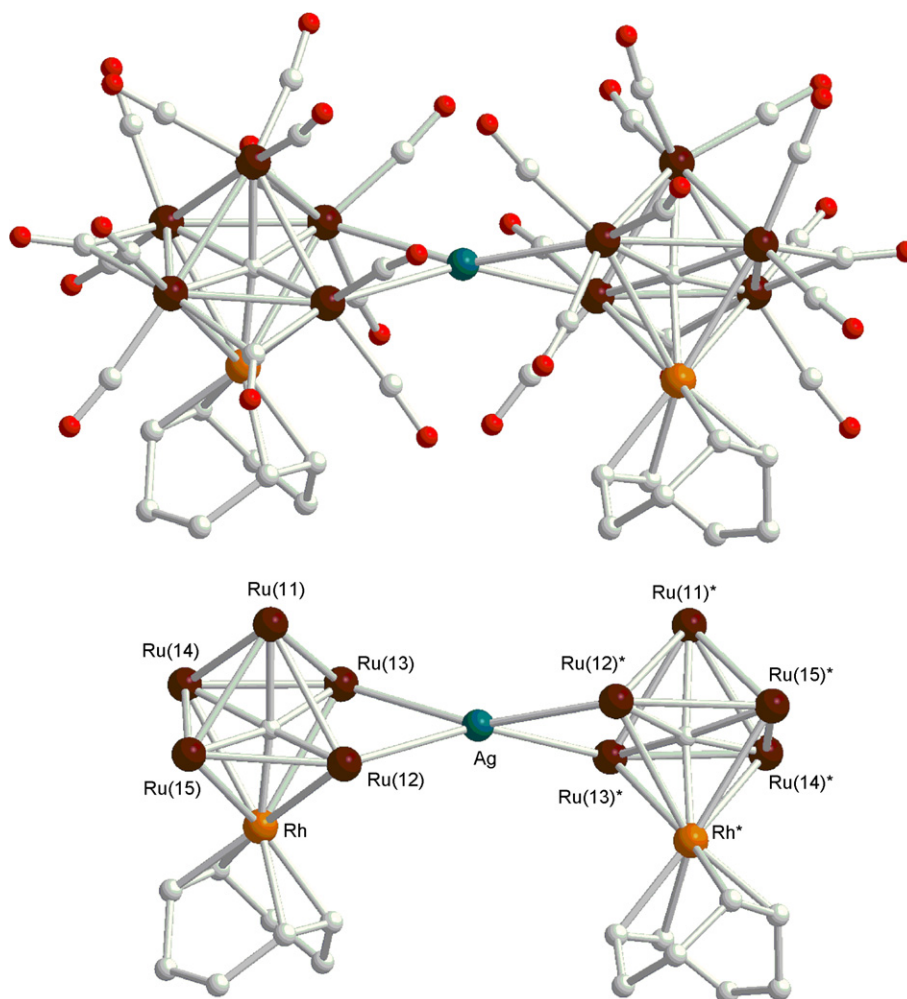


Fig. 1. Crystal structure of the cluster anion of **2** (top). The figure at the bottom omits CO ligands for simplicity.

Table 1
Selected bond lengths (Å) and angles (°) for [PPN][Ag[RhRu₅C(CO)₁₄(cod)]₂ (**2**)

Bond lengths (Å)			
Ag–Ru(12)	2.9118(2)	Ag–Ru(13)	2.9293(4)
Rh–Ru(12)	2.9218(2)	Ru(11)–Ru(12)	2.9191(5)
Rh–Ru(13)	3.0387(4)	Ru(11)–Ru(13)	2.8776(3)
Rh–Ru(14)	2.9556(5)	Ru(11)–Ru(14)	2.8265(6)
Rh–Ru(15)	2.9392(4)	Ru(11)–Ru(15)	2.8494(4)
Ru(12)–Ru(13)	3.0747(5)	Ru(13)–Ru(14)	2.8698(4)
Ru(12)–Ru(15)	2.8459(4)	Ru(14)–Ru(15)	2.8418(5)
Bond angles (°)			
Ru(12)–Ag–Ru(13)	63.985(9)	Ru(12)–Ag–Ru(12)*	154.50(2)
Ru(12)–Ag–Ru(13)*	121.971(10)	Ru(13)–Ag–Ru(13)*	156.24(2)
Ag–Ru(12)–Ru(11)	96.27(1)	Ag–Ru(13)–Ru(11)	96.79(2)
Ag–Ru(12)–Ru(13)	58.284(8)	Ag–Ru(13)–Ru(12)	57.73(1)
Ag–Ru(12)–Rh	99.71(1)	Ag–Ru(13)–Rh	96.68(2)

Interestingly a similar reaction of the rhodium–ruthenium carbonyl cluster that does not have cyclooctadiene ligand, [PPN][RhRu₅C(CO)₁₆] (**3**), with 0.5 AgNO₃ did not afford the corresponding silver bridged complex, but starting material **3** was recovered quantitatively. The $\nu(\text{CO})$ in **3** appeared at 2021 cm⁻¹, which is 28 cm⁻¹ higher than that in **1** indicating that replacement of the cyclic diene unit with two CO ligands leads to decrease of electronic charge of the RhRu₅ cluster core. Presumably, the silver cation distinguishes this difference and thus showed no affinity towards complex **3**.

2.2. Synthesis of {Ag₂[CuRu₆C(CO)₁₆Cl]₂}²⁻ cluster complex

The hexanuclear ruthenium carbido anion [PPh₄]₂[Ru₆C(CO)₁₆] was reacted with an equivalent amount of CuCl in THF at room temperature for 12 h. On evaporation of the solvent, dark red crystals were obtained in excellent yield, the elemental analysis of which was consistent to the composition [PPh₄]₂[CuRu₆C(CO)₁₆Cl] (**4**). Its IR spectra has the $\nu(\text{CO})$ band at 1993 cm⁻¹. The shift to higher energy by 20 cm⁻¹ as compared to the parent carbonyl cluster indicates the strong electron-withdrawing nature of the CuCl group. The structure of **4** has been confirmed by single-crystal X-ray analysis as shown in Fig. 2. The Cu atom caps one of the trigonal faces of the Ru₆ core and therefore has three Cu–Ru bonds ranging from 2.6434(12) to 2.7082(10) Å (Table 2). Within the Ru₆ octahedron the three Ru–Ru edges that are capped by the Cu atom are slightly longer (average 2.95 Å) than the other nine edges (average 2.90 Å).

Treatment of **4** with one equivalent of AgNO₃ in THF at room temperature for 12 h gave dark red crystals of the composition [PPh₄]₂{Ag₂[CuRu₆C(CO)₁₆Cl]₂} (**5**) in 72% yield. The molecular structure of the anionic part of **5**, established by X-ray crystal analysis, is shown in Fig. 3 while the important bond lengths and angles are listed in Table 3. Although the unit cell contained three independent units, structural parameters for only one of them are

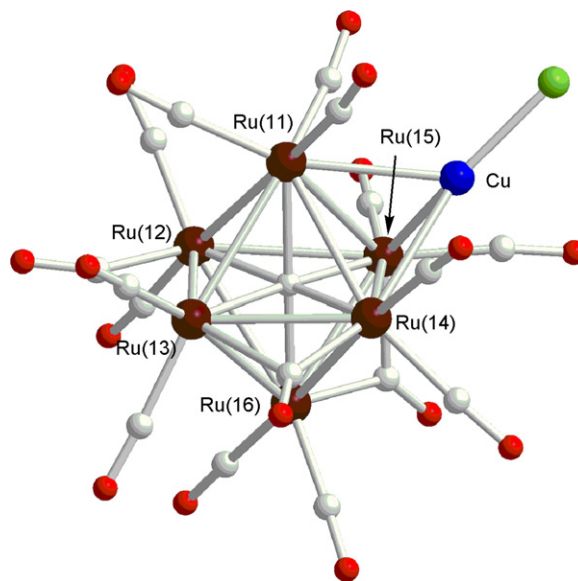


Fig. 2. Structure of the cluster anion of **4** in the crystal.

given since the differences between the three are very small. The overall structure of the anion in **5** is similar but more distorted compared to that of anion in [PPh₄]₂{Cu₄[Ru₆C(CO)₁₆]₂Cl₂} (**6**), which was prepared by the reaction of [PPh₄]₂[Ru₆C(CO)₁₆] with five equivalents of CuCl [6]. The anionic cluster molecule has a crystallographic center of symmetry at the center of the Ag₂Cu₂ plane. The Ru₆C–CuCl unit in **5** retains its original metal core geometry of the precursor dianion **4**. The chloride-bridged Ag–Cu bond distances are 0.31 Å longer than the Ag–Cu bonds, that interact with the Ru cluster core. Ag₂Cu₂ framework is therefore parallelogram, Cu–Ag–Cu* 110.63(4), Ag–Cu–Ag* 69.38(3)° in contrast to almost square Cu₄ plane in **6**.

Table 2
Selected bond lengths (Å) and angles (°) for [PPh₄]₂[CuRu₆C(CO)₁₆Cl] (**4**)

Bond lengths (Å)			
Cu–Ru(11)	2.7053(11)	Cu–Ru(14)	2.7082(10)
Cu–Ru(15)	2.6434(12)	Cu–Cl	2.166(2)
Ru(11)–Ru(12)	2.8454(9)	Ru(12)–Ru(16)	2.9660(9)
Ru(11)–Ru(13)	2.9563(8)	Ru(13)–Ru(14)	2.8472(8)
Ru(11)–Ru(14)	2.9014(7)	Ru(13)–Ru(16)	2.9312(9)
Ru(11)–Ru(15)	2.9876(8)	Ru(14)–Ru(15)	2.9654(8)
Ru(12)–Ru(13)	2.8276(10)	Ru(14)–Ru(16)	2.9245(8)
Ru(12)–Ru(15)	2.9985(8)	Ru(15)–Ru(16)	2.7955(9)
Bond angles (°)			
Ru(11)–Cu–Ru(14)	64.82(2)	Ru(11)–Cu–Cl	129.45(7)
Ru(11)–Cu–Ru(15)	67.90(2)	Ru(14)–Cu–Cl	152.92(7)
Ru(14)–Cu–Ru(15)	67.29(2)	Ru(15)–Cu–Cl	136.72(7)
Cu–Ru(11)–Ru(14)	57.64(2)	Cu–Ru(14)–Ru(11)	57.54(2)
Cu–Ru(11)–Ru(15)	55.06(2)	Cu–Ru(14)–Ru(15)	55.32(2)
Ru(14)–Ru(11)–Ru(15)	60.45(2)	Ru(11)–Ru(14)–Ru(15)	61.22(2)
Cu–Ru(15)–Ru(11)	57.01(2)	Cu–Ru(15)–Ru(14)	57.40(2)
Ru(11)–Ru(15)–Ru(14)	58.34(2)		

2.3. Syntheses of $\{Cu_4Pd_2[Ru_6C(CO)_{16}]_2Cl_2\}^{2-}$, $\{Pt_2[Ru_6C(CO)_{16}]_2\}^{2-}$, and $\{Cu_7[Ru_6C(CO)_{15}]_2Cl_3\}^{2-}$ complexes

The reaction of ruthenium–copper cluster **4** with one equivalent $[Pd(CH_3CN)_4]BF_4$ in THF at room temperature for 12 h afforded dark-red crystals of $[PPh_4]_2\{Cu_4Pd_2[Ru_6C(CO)_{16}]_2Cl_2\}$ (**7**) as confirmed by X-ray structural analysis (Fig. 4; Table 4). The yield, however, was very low and the reproducibility of the reaction was poor. We noticed that this three component Cu–Pd–Ru might be produced by incorporation of two Pd(0) atoms into the copper–ruthenium mixed-metal cluster **6**. In accord with this hypothesis, the reaction of **6** with an equimolar amount of $Pd_2(dba)_3 \cdot CHCl_3$ and work up on a silica gel column gave complex **7** in fairly good yield and with good reproducibility. The crystal structure of the anionic cluster **7** has a crystallographic center of symmetry at the center of the molecule (mid point between Pd–Pd*). The $Ru_{12}Cu_4$ skeleton retains its original geometry in **6** except that the Cu(1)–Cu(2) and Cu(2)–Ru(14) bonds are broken while Cu(2)–Ru(16) bond forms; the Cu(1)–Cu(2), Cu(2)–Ru(14), and Cu(2)–Ru(16) distances are 4.311(2), 3.700(2), and 2.628(2) Å, respectively. The whole structure may be viewed as the linear edge-condensation of four octahedrons, two $[Ru_6C]$ and two $[Ru_2Pd_2Cu_2]$ skeletons, if some long metal–metal distances are taken as edges.

Each palladium atom has one homometallic Pd–Pd* bond and five heterometallic bonds, three to three copper atoms, two to the broken Ru–Ru edges (nonbonded Pd–Cu(1)* distance 3.180(1) Å). Cu(1) has one homometallic Cu(1)–Cu(2)* bond and four heterometallic bonds, three to the ruthenium atoms of the broken Ru(14)–Ru(15) edge and one to apical ruthenium atom and one to Pd atom. On the other hand, Cu(2) has one homometallic Cu(2)–Cu(1)* bond and four heterometallic bonds, two to Pd and Pd* atoms and two to Ru(15) and Ru(16) atoms.

When cluster **6** in THF was reacted with zero-valent platinum species $Pt(dba)_2$ at room temperature for 12 h, subsequent chromatography on a silica gel column of the reaction mixture gave dark red crystals which were not the expected analog of **7**, but found to be a platinum–ruthenium hetero bimetallic cluster of the formula $[PPh_4]_2\{Pt_2[Ru_6C(CO)_{15}]_2\}$ (**8**) obtained in 30% yield. The structure of anion $\{Pt_2[Ru_6C(CO)_{15}]_2\}^{2-}$, as determined by single-crystal X-ray analysis (Fig. 5; Table 5), is similar to that of mixed-metal palladium–ruthenium cluster $[PPN]_2\{Pd_2[Ru_6C(CO)_{15}]_2\}$ prepared from $[Ru_6C(CO)_{16}]^{2-}$ and $[Pd(CH_3CN)_4]^{2+}$ in the air [29]. There is a crystallographic center of symmetry at the center of the anion in **8** (mid point between Pt–Pt*). The two Pt atoms bridge two Ru_6 moieties by capping the trigonal faces. Each Pt atom has, therefore, six Pt–Ru bonds ranging from 2.7118(7) to 2.7726(6) Å. As in the case of the Pd analogue,

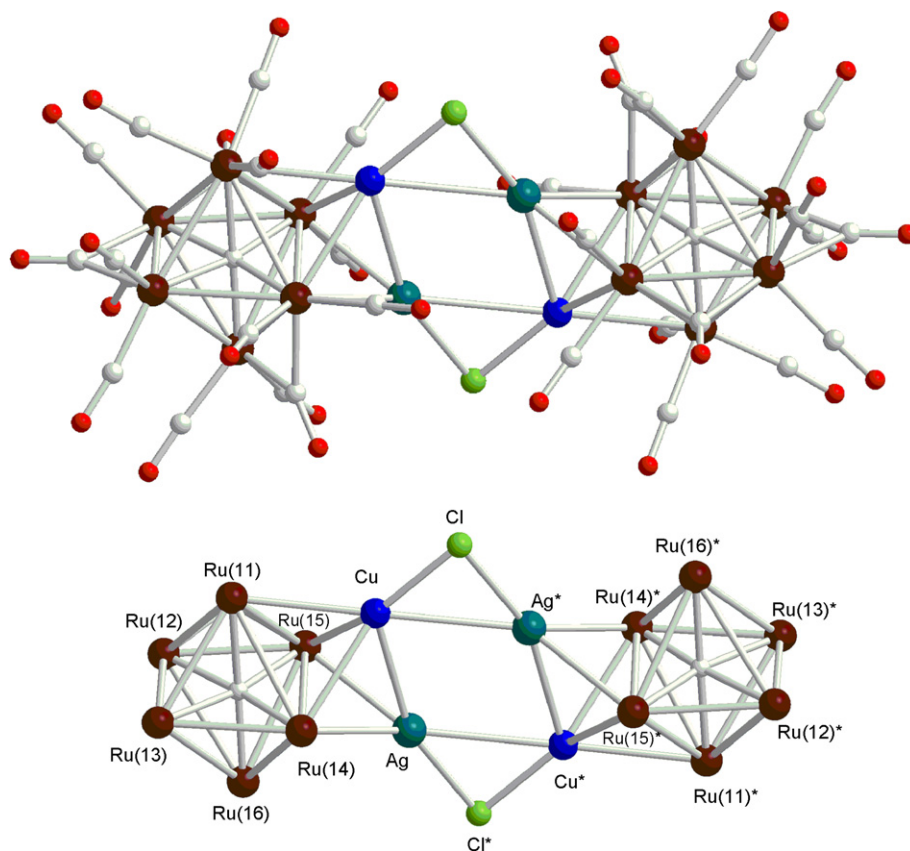


Fig. 3. Crystal structure of the cluster anion of **5** (top). The figure at the bottom omits CO ligands for simplicity.

Table 3

Selected bond lengths (Å) and angles (°) for $[\text{PPh}_4]_2[\text{Ag}_2\{\text{CuRu}_6\text{C}(\text{CO})_{16}\}_2\text{Cl}_2]$ (**5**)

Bond lengths (Å)			
Ag–Cu	2.700(2)	Ag–Cu*	3.013(1)
Ag–Ru(14)	2.769(1)	Ag–Ru(15)	2.832(1)
Ag–Ru(16)	3.580(1)	Ag–Cl*	2.419(3)
Cu–Ru(11)	2.788(1)	Cu–Ru(14)	2.708(1)
Cu–Ru(15)	2.718(2)	Cu–Cl	2.220(3)
Ru(11)–Ru(12)	2.856(1)	Ru(11)–Ru(13)	2.898(1)
Ru(11)–Ru(14)	2.913(1)	Ru(11)–Ru(15)	2.976(1)
Ru(12)–Ru(13)	2.842(1)	Ru(12)–Ru(15)	2.876(1)
Ru(12)–Ru(16)	2.918(1)	Ru(13)–Ru(14)	2.789(1)
Ru(13)–Ru(16)	2.973(1)	Ru(14)–Ru(15)	3.157(1)
Ru(14)–Ru(16)	2.944(1)	Ru(15)–Ru(16)	2.816(1)
Bond angles (°)			
Cu–Ag–Cu*	110.63(4)	Ag–Cu–Ag*	69.38(3)
		Ru(11)–Cu–Cl	125.49(10)
Ru(14)–Ag–Cl*	137.14(7)	Ru(14)–Cu–Cl	143.13(9)
Ru(15)–Ag–Cl*	136.45(8)	Ru(15)–Cu–Cl	145.37(9)
Cu–Ag–Cl*	157.29(8)	Ag–Cu–Cl	121.80(9)

Table 4

Selected bond lengths (Å) and angles (°) for $[\text{PPh}_4]_2\{\text{Cu}_4\text{Pd}_2[\text{Ru}_6\text{C}(\text{CO})_{16}\}_2\text{Cl}_2\}$ (**7**)

Bond lengths (Å)			
Pd–Pd*	2.633(2)		
Pd–Ru(14)	2.740(2)	Pd–Ru(15)*	2.766(2)
Pd–Cu(1)	2.677(2)	Pd–Cu(2)	2.784(2)
Pd–Cu(1)*	3.180(2)	Pd–Cu(2)*	2.968(2)
Cu(1)–Cu(2)	4.311(2)	Cu(1)–Cu(2)*	2.885(2)
Cu(1)–Ru(11)	2.813(2)	Cu(2)–Ru(16)	2.628(2)
Cu(1)–Ru(14)	2.757(2)	Cu(2)–Ru(14)	3.700(2)
Cu(1)–Ru(15)	2.671(2)	Cu(2)–Ru(15)	2.681(2)
Cu(1)–Cl	2.228(3)	Cu(2)–Cl*	2.234(5)
Ru(14)–Ru(15)	3.165(2)		
Bond angles (°)			
Ru(14)–Pd–Ru(15)*	165.09(6)	Pd*–Pd–Ru(14)	116.90(5)
Pd*–Pd–Cu(1)	73.58(5)	Pd*–Pd–Cu(2)	66.38(4)
Pd*–Pd–Cu(2)*	59.26(4)	Cu(1)–Pd–Cu(2)	104.24(6)
Cu(1)–Pd–Ru(14)	61.16(4)	Cu(1)–Pd–Ru(15)*	116.89(4)
Cu(2)–Pd–Ru(14)	84.08(5)	Cu(2)–Pd–Ru(15)*	110.21(6)
Cu(2)*–Pd–Ru(14)	119.87(6)	Cu(2)*–Pd–Ru(15)*	55.63(4)

the atoms Ru(14) and Ru(15) (and Ru(14)* and Ru(15)*) are interacting with the two bridging Pt metal atoms and thus no longer bonded to each other, the Ru–Ru distance being 3.2785(7) Å.

A silver analog of Cu–Ru heterometallic cluster **6**, $[\text{PPN}]_2\{\text{Ag}_4[\text{Ru}_6\text{C}(\text{CO})_{16}\}_2\text{Cl}_2\}$ (**6'**) [6] reacted smoothly with two equivalents $\text{Pd}_2(\text{dba})_3 \cdot \text{CHCl}_3$ in THF at room temperature for 12 h. The product was not an expected

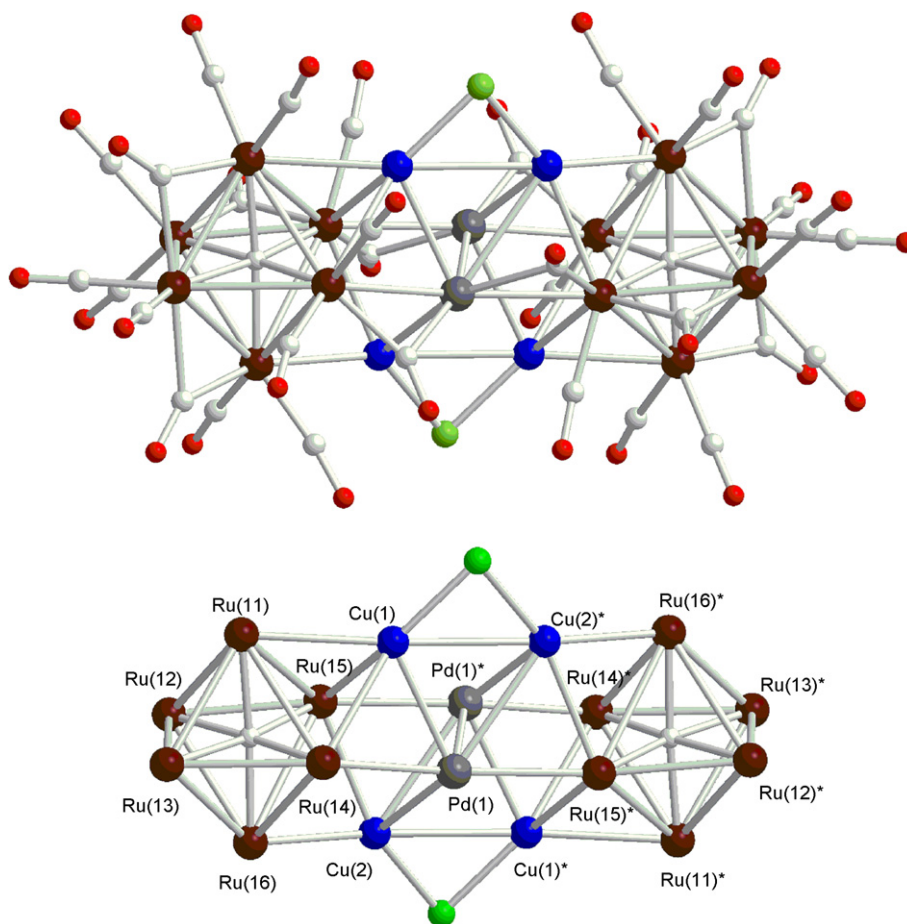


Fig. 4. Crystal structure of the cluster anion of **7** (top). The figure at the bottom omits CO ligands for simplicity.

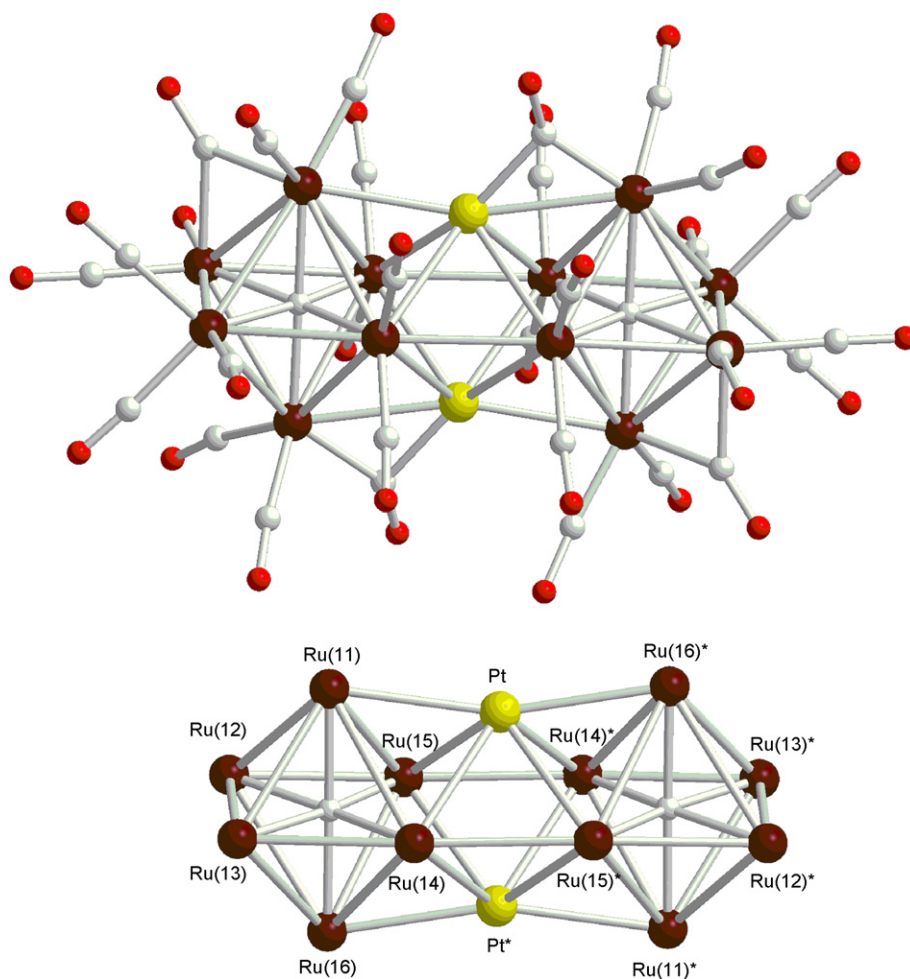


Fig. 5. Crystal structure of the cluster anion of **8** (top). The figure at the bottom omits CO ligands for simplicity.

Table 5
Selected bond lengths (Å) and angles (°) for $[\text{PPh}_4]_2\{\text{Pt}_2[\text{Ru}_6\text{C}(\text{CO})_{15}]_2\}$ (**8**)

Bond lengths (Å)			
Pt–Ru(11)	2.7534(5)	Pt*–Ru(14)	2.7694(6)
Pt–Ru(14)	2.7118(7)	Pt*–Ru(15)	2.7356(4)
Pt–Ru(15)	2.7255(5)	Pt*–Ru(16)	2.7726(6)
Ru(14)–Ru(15)*	2.8721(7)		
Ru(11)–Ru(12)	2.9198(7)	Ru(11)–Ru(13)	3.0439(9)
Ru(11)–Ru(14)	2.9274(5)	Ru(11)–Ru(15)	2.9523(8)
Ru(12)–Ru(13)	2.8094(5)	Ru(12)–Ru(15)	2.8572(7)
Ru(12)–Ru(16)	2.9368(5)	Ru(13)–Ru(14)	2.8378(7)
Ru(13)–Ru(16)	2.8389(8)	Ru(14)–Ru(15)	3.2785(7)
Ru(14)–Ru(16)	2.9158(7)	Ru(15)–Ru(16)	2.9591(9)
Bond angles (°)			
Ru(11)–Pt–Ru(16)*	162.77(2)	Ru(14)–Pt–Ru(15)*	63.64(2)
Ru(14)–Pt–Ru(15)	74.17(2)	Ru(14)*–Pt–Ru(15)*	73.11(2)
Ru(15)–Pt–Ru(14)*	63.02(2)	Pt–Ru(15)–Pt*	74.53(2)
Pt–Ru(14)–Pt*	74.21(2)		

Ag analog of **7**, but turned out to be a palladium–ruthenium bimetallic cluster of the formula $[\text{PPN}]_2\{\text{Pd}_4[\text{Ru}_6\text{C}(\text{CO})_{16}]_2\}$ (**9**) isolated in 71% yield. The same complex was previously obtained from the reaction of $[\text{Ru}_6\text{C}(\text{CO})_{16}]^{2-}$ and $[\text{Pd}(\text{CH}_3\text{CN})_4]^{2+}$ in 34% yield [29]. It is noteworthy that Pd(0) and Pt(0) species are partly oxi-

dized during the formation of **8** and **9**, while such a redox process does not take place in the reaction of Pd(0) with **6** to give **7**.

Treatment of **6** with an equimolar amount of $[\text{RhCl}(\text{CO})_2]_2$ in THF at room temperature for 12 h gave two complexes after silica gel chromatography: the known cluster $[\text{PPh}_4][\text{RhRu}_5\text{C}(\text{CO})_{16}]$ [38] (36%) and a new dark-red crystalline complex, $[\text{PPh}_4]_2\{\text{Cu}_7[\text{Ru}_6\text{C}(\text{CO})_{15}]_2\text{Cl}_3\}$ (**10**) (24% yield based on the starting cluster complex). The structure of **10**, determined by single-crystal X-ray diffraction analysis, is shown in Fig. 6 and important bond lengths and angles are given in Table 6. The central Cu_7 core forms two fused square pyramids. A similar Cu_7 core, which is flanked on each side by tetrahedral Ru_4 has been found in $\{\text{Cu}_7[\text{Ru}_4\text{H}(\text{CO})_{12}]_2\text{Cl}_3\}^{2-}$ [5]. The cluster anion has two pseudo-mirror planes, one of which passes Cu(2), Cu(5), Ru(13), and Ru(23) and the other through Cu(1), Cu(2), Cu(3), and Cu(7). Three chloro ligands bridge three pairs of the Cu atoms in the core. The remaining Cu atom, Cu(7), has eight bonds, six to the other Cu atom and two to Ru(15) and Ru(25). The three chloro-bridged edges are significantly longer (average 2.94 Å) than the other 10 edges (average 2.57 Å).

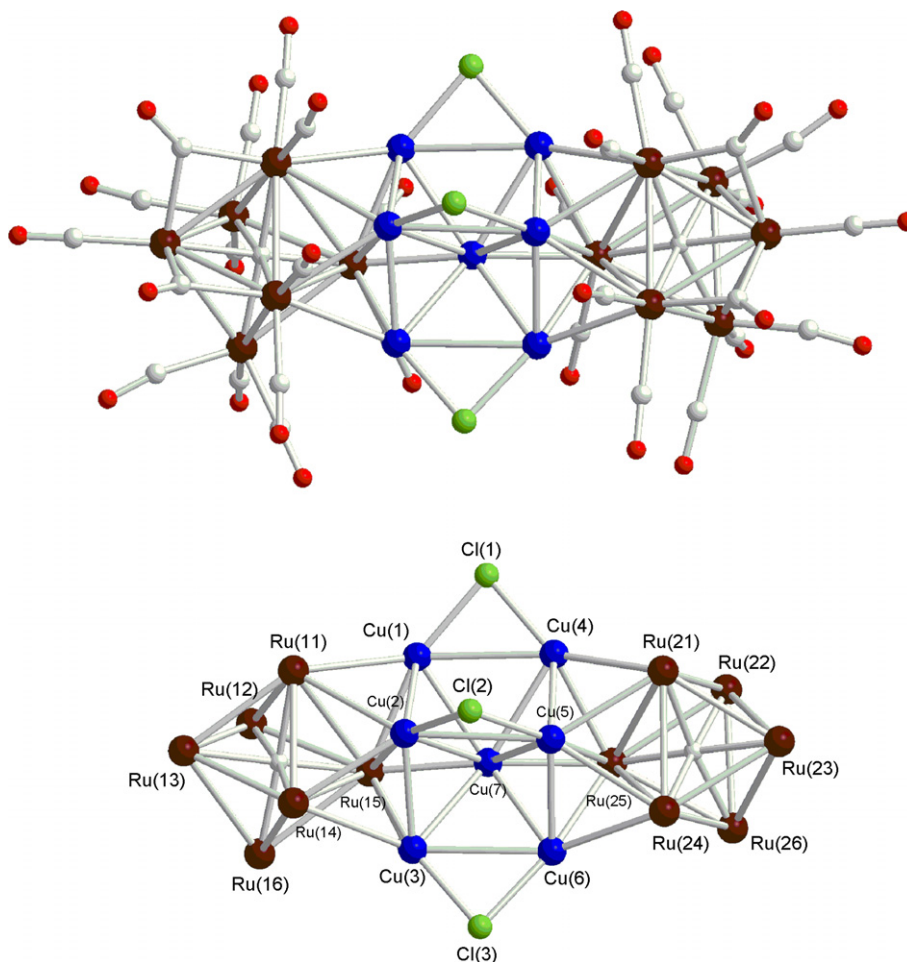


Fig. 6. Crystal structure of the cluster anion of **10** (top). The figure at the bottom omits CO ligands for simplicity.

3. Summary

High nuclearity cluster complexes comprising of three different transition metals (Ag, Rh, Ru), (Ag, Cu, Ru), and (Cu, Ru, Pd) were synthesized by the ionic coupling reaction of two-component clusters with third metals. In addition, two new two-component mixed-metal carbonyl clusters (Pt, Ru), (Cu, Ru) were prepared.

4. Experimental

All reactions were carried out in dry solvents under purified argon. Solvents were purified by standard methods and freshly distilled from Na-benzophenone or CaH₂ under argon before use. The starting materials and complexes [PPN]₂[Ru₅C(CO)₁₄] [39], [PPh₄]₂[Ru₆C(CO)₁₆] [40], [Rh(cod)(NH₃)₂PF₆] [41], Pd₂(dba)₃ · CHCl₃ [42], Pt(dba)₂ [43], [RhCl(CO)₂]₂ [44], and [PPh₄]₂{Cu₄[Ru₆C(CO)₁₆]-Cl₂} [6] were obtained by published procedures. All other reagents were commercially obtained. ¹H NMR spectra were measured on a JEOL EX-270 spectrometer and IR spectra were recorded on a Perkin–Elmer FT-1650 spectrometer using a CaF₂ liquid cell. All data collections for X-ray analysis were made on a Rigaku RAXIS-RAPID

Imaging Plate diffractometer with graphite-monochromated Mo K α ($\lambda = 0.71073$ Å) radiation except for **7**. Reflection data for **7** were collected on a CAD-4 diffractometer using graphite-monochromated Mo K α ($\lambda = 0.71073$ Å) and ω - 2θ scan technique. Crystallographic data are given in Tables 7 and 8. Structures were solved by direct methods, expanded using Fourier techniques, and refined by full-matrix least-squares. All calculations were performed using the teXsan crystallographic software package of Molecular Structure Corporation (1992). All non-hydrogen atoms were refined with anisotropic atomic displacement parameters (anisotropically) except for the acetone unit contained in **10** as solvent of crystallization. All hydrogen atoms were placed in idealized positions, assigned isotropic displacement parameters and allowed to ride on the parent carbons.

4.1. Synthesis of [PPN]₂{Ag[RhRu₅C(CO)₁₄(cod)]₂} (**2**)

A mixture of [PPN][RhRu₅C(CO)₁₄(cod)] (**1**) (82.7 mg, 0.050 mmol) and AgNO₃ (4.2 mg, 0.025 mmol) in THF (20 ml) was stirred at room temperature for 12 h. The solvent was evaporated under reduced pressure and the residual dark-red solid was chromatographed on SiO₂

Table 6
Selected bond lengths (Å) and angles (°) for $[\text{PPh}_4]_2\{\text{Cu}_7[\text{Ru}_6\text{C}(\text{CO})_{15}]_2\text{Cl}_3\}$ (**10**)

Bond lengths (Å)			
Cu(1)–Cu(2)	2.491(1)	Cu(2)–Cu(3)	2.478(1)
Cu(1)–Cu(4)	2.880(1)	Cu(2)–Cu(5)	3.047(1)
Cu(1)–Cu(7)	2.607(1)	Cu(2)–Cu(7)	2.597(1)
Cu(1)–Ru(11)	2.739(1)	Cu(2)–Ru(11)	2.797(1)
Cu(1)–Ru(15)	2.637(1)	Cu(2)–Ru(14)	2.725(1)
Cu(1)–Cl(1)	2.222(2)	Cu(2)–Ru(15)	2.719(1)
Cu(3)–Cu(6)	2.883(1)	Cu(2)–Cl(2)	2.221(2)
Cu(3)–Cu(7)	2.663(1)	Cu(4)–Cu(5)	2.483(1)
Cu(3)–Ru(14)	2.754(1)	Cu(4)–Cu(7)	2.663(1)
Cu(3)–Ru(15)	2.628(1)	Cu(4)–Ru(21)	2.738(1)
Cu(3)–Cl(3)	2.216(2)	Cu(4)–Ru(25)	2.635(1)
Cu(5)–Cu(6)	2.492(1)	Cu(4)–Cl(1)	2.213(2)
Cu(5)–Cu(7)	2.582(1)	Cu(6)–Cu(7)	2.634(1)
Cu(5)–Ru(21)	2.716(1)	Cu(6)–Ru(24)	2.724(1)
Cu(5)–Ru(24)	2.828(1)	Cu(6)–Ru(25)	2.633(1)
Cu(5)–Ru(25)	2.720(1)	Cu(6)–Cl(3)	2.218(2)
Cu(5)–Cl(2)	2.229(2)		
Bond angles (°)			
Cu(4)–Cu(1)–Ru(11)	149.16(3)	Cu(1)–Cu(4)–Ru(21)	153.82(4)
Cu(2)–Cu(1)–Cu(4)	89.36(2)	Cu(1)–Cu(4)–Cu(5)	94.19(3)
Cu(2)–Cu(1)–Cu(7)	61.19(3)	Cu(5)–Cu(4)–Cu(7)	60.11(3)
Cu(4)–Cu(1)–Cu(7)	57.82(2)	Cu(1)–Cu(4)–Cu(7)	55.94(2)
Cu(1)–Cu(2)–Cu(3)	113.89(3)	Cu(4)–Cu(5)–Cu(6)	114.49(3)
Cu(1)–Cu(2)–Cu(7)	61.61(3)	Cu(4)–Cu(5)–Cu(7)	63.41(3)
Cu(3)–Cu(2)–Cu(7)	63.23(3)	Cu(6)–Cu(5)–Cu(7)	62.51(2)
Cu(6)–Cu(3)–Ru(14)	154.83(4)	Cu(3)–Cu(6)–Ru(24)	149.76(4)
Cu(2)–Cu(3)–Cu(6)	95.11(3)	Cu(3)–Cu(6)–Cu(5)	88.43(3)
Cu(2)–Cu(3)–Cu(7)	60.55(3)	Cu(5)–Cu(6)–Cu(7)	60.42(2)
Cu(6)–Cu(3)–Cu(7)	56.54(2)	Cu(3)–Cu(6)–Cu(7)	57.49(2)

(deactivated with 10 wt% H_2O). The dark-red solution eluted with CH_2Cl_2 was collected and evaporated to dryness to yield dark-red solid of **2** (59.5 mg, 0.021 mmol, 82% yield). Analytically pure sample was obtained by recrystallization from CH_2Cl_2 –MeOH as dark-red plates. IR $\nu(\text{CO})$ 2062 (m), 2054(m), 2022(vs), 1999(s) cm^{-1} . Anal. Calc. for $\text{C}_{82}\text{H}_{54}\text{AgNO}_{28}\text{P}_2\text{Rh}_2\text{Ru}_{10}$: C, 34.11; H, 1.88; N, 0.49. Found: C, 34.04; H, 1.86; N, 0.39%. ^1H NMR (270 MHz, CDCl_3) σ 4.76 (bs, 8H), 2.19 (bs, 8H), 1.79 (bs, 8H).

4.2. Synthesis of $[\text{PPh}_4]_2[\text{CuRu}_6\text{C}(\text{CO})_{16}\text{Cl}]$ (**4**)

A mixture of $[\text{PPh}_4]_2[\text{Ru}_6\text{C}(\text{CO})_{16}]$ (100 mg, 0.057 mmol) and CuCl (5.7 mg, 0.057 mmol) in THF (20 ml) was stirred at room temperature for 12 h. The initially red solution became dark red in color. The reaction mixture was filtered through Celite before drying under vacuum, the residual red solid was crystallized from CH_2Cl_2 –MeOH to give **4** (86.5 mg, 0.047 mmol, 82%). IR $\nu(\text{CO})$ 1993(s) cm^{-1} . Anal. Calc. for $\text{C}_{65}\text{H}_{40}\text{ClCuO}_{16}\text{P}_2\text{Ru}_6$: C, 42.33; H, 2.19, N, 0.00. Found: C, 42.10; H, 2.11, N, 0.00%.

4.3. Synthesis of $[\text{PPh}_4]_2\{\text{Ag}_2[\text{CuRu}_6\text{C}(\text{CO})_{16}]_2\text{Cl}_2\}$ (**5**)

A mixture of $[\text{PPh}_4]_2[\text{CuRu}_6\text{C}(\text{CO})_{16}\text{Cl}]$ (**4**) (86.5 mg, 0.047 mmol) and AgNO_3 (7.9 mg, 0.047 mmol) in THF

(20 ml) was stirred at room temperature for 12 h. The reaction mixture was filtered through Celite before drying under vacuum, the residual red solid was crystallized from CH_2Cl_2 /MeOH to give **5** (53.9 mg, 0.017 mmol, 72%). Analytically pure sample was obtained by recrystallization from CH_2Cl_2 –MeOH as dark-red plates. IR $\nu(\text{CO})$ 2055(m), 2023(s) cm^{-1} . Anal. Calc. for $\text{C}_{82}\text{H}_{40}\text{Ag}_2\text{Cl}_2\text{Cu}_2\text{O}_{32}\text{P}_2\text{Ru}_{12}$: C, 30.53; H, 1.25, N, 0.00. Found: C, 30.45; H, 1.20, N, 0.00%.

4.4. Synthesis of $[\text{PPh}_4]_2\{\text{Cu}_4\text{Pd}_2[\text{Ru}_6\text{C}(\text{CO})_{16}]_2\text{Cl}_2\}$ (**7**)

A mixture of $[\text{PPh}_4]_2\{\text{Cu}_4[\text{Ru}_6\text{C}(\text{CO})_{16}]_2\text{Cl}_2\}$ (120 mg, 0.038 mmol) and $\text{Pd}_2(\text{dba})_3 \cdot \text{CHCl}_3$ (38 mg, 0.038 mmol) was stirred at room temperature for 12 h. The solvent was evaporated under reduced pressure and the residual dark-red solid was chromatographed on SiO_2 (deactivated with 10 wt% H_2O). The dark-red solution eluted with CH_2Cl_2 /THF (9/1) was collected and evaporated to dryness to yield dark-red solid of **7** (80.4 mg, 0.024 mmol, 62%). Analytically pure sample was obtained by recrystallization from acetone–MeOH as dark-red plates. IR $\nu(\text{CO})$ 2045 (m), 2021(s) cm^{-1} . Anal. Calc. for $\text{C}_{82}\text{H}_{40}\text{Cl}_2\text{Cu}_4\text{O}_{32}\text{Pd}_2\text{P}_2\text{Ru}_{12}$: C, 29.40; H, 1.20, N, 0.00. Found: C, 29.18; H, 1.18, N, 0.00%.

4.5. Synthesis of $[\text{PPh}_4]_2\{\text{Pt}_2[\text{Ru}_6\text{C}(\text{CO})_{15}]_2\}$ (**8**)

A mixture of $[\text{PPh}_4]_2\{\text{Cu}_4[\text{Ru}_6\text{C}(\text{CO})_{16}]_2\text{Cl}_2\}$ (50 mg, 0.016 mmol) and $\text{Pt}(\text{dba})_2$ (21 mg, 0.032 mmol) was stirred at room temperature for 12 h. The solvent was evaporated under reduced pressure and the residual dark-red solid was chromatographed on SiO_2 (deactivated with 10 wt% H_2O). The dark-red solution eluted with CH_2Cl_2 /THF (9/1) was collected and evaporated to dryness to yield dark-red solid of **8** (15.0 mg, 0.005 mmol, 30%). Analytically pure sample was obtained by recrystallization from acetone–MeOH as dark-red plates. IR $\nu(\text{CO})$ 2021(s) cm^{-1} . Anal. Calc. for $\text{C}_{80}\text{H}_{40}\text{O}_{30}\text{P}_2\text{Pt}_2\text{Ru}_{12}$: C, 30.54; H, 1.28. Found: C, 30.47, N, 0.00; H, 1.19, N, 0.00%.

4.6. Synthesis of $[\text{PPN}]_2\{\text{Pd}_4[\text{Ru}_6\text{C}(\text{CO})_{16}]_2\}$ (**9**)

A mixture of $[\text{PPh}_4]_2\{\text{Ag}_4[\text{Ru}_6\text{C}(\text{CO})_{16}]_2\text{Cl}_2\}$ (50 mg, 0.013 mmol) and $\text{Pd}_2(\text{dba})_3 \cdot \text{CHCl}_3$ (26 mg, 0.026 mmol) was stirred at room temperature for 12 h. The solvent was evaporated under reduced pressure and the residual dark-red solid was chromatographed on SiO_2 (deactivated with 10 wt% H_2O). The dark-red solution eluted with CH_2Cl_2 was collected and evaporated to dryness to yield dark-red solid of **9** (33.6 mg, 0.009 mmol, 71%).

4.7. Synthesis of $[\text{PPh}_4]_2\{\text{Cu}_7[\text{Ru}_6\text{C}(\text{CO})_{15}]_2\text{Cl}_3\}$ (**10**)

A mixture of $[\text{PPh}_4]_2\{\text{Cu}_4[\text{Ru}_6\text{C}(\text{CO})_{16}]_2\text{Cl}_2\}$ (183 mg, 0.059) and $[\text{RhCl}(\text{CO})_2]_2$ (23 mg, 0.059 mmol) was stirred at room temperature for 12 h. The initially red solution

Table 7

Crystallographic data for complexes [PPN][AgRhRu₅C(CO)₁₄(cod)]₂ (**2**), [PPh₄]₂[CuRu₆C(CO)₁₆Cl] (**4**), and [PPh₄]₂[Ag₂[CuRu₆C(CO)₁₆]₂Cl₂] (**5**)

Compound	2	4	5
Formula	C ₈₂ H ₅₄ AgNO ₂₈ P ₂ Rh ₂ Ru ₁₀	C ₆₅ H ₄₀ ClCuO ₁₆ P ₂ Ru ₆	3(C ₈₂ H ₄₀ Ag ₂ Cl ₂ Cu ₂ O ₃₂ P ₂ Ru ₁₂) · 2(CH ₂ Cl ₂)
Formula weight	2887.65	1844.39	9846.33
Crystal system	Monoclinic	Monoclinic	Triclinic
Space group	C2/c	P2 ₁ /n	P $\bar{1}$
<i>a</i> (Å)	30.404(9)	12.405(2)	19.7997(9)
<i>b</i> (Å)	19.227(6)	14.661(2)	20.7642(9)
<i>c</i> (Å)	18.987(4)	36.426(5)	18.6161(9)
α (°)			99.253(1)
β (°)	127.74(1)	94.940(7)	97.133(1)
γ (°)			76.909(1)
<i>V</i> (Å ³)	8778(4)	6600(2)	7326.9(6)
<i>Z</i>	4	4	1
Crystal size (mm)	0.28 × 0.15 × 0.07	0.31 × 0.24 × 0.11	0.35 × 0.22 × 0.10
<i>T</i> (K)	300	300	300
<i>D</i> _{calc} (g cm ⁻³)	2.185	1.85	2.23
μ (cm ⁻¹)	23.63	18.05	28.11
Full-matrix least-square	<i>F</i> ²	<i>F</i> ²	<i>F</i> ²
Reflections collected	22338	35572	78076
Unique reflections	9938	15566	39328
Reflections observed [<i>I</i> > 2 σ (<i>I</i>)]	6312	7170	25700
<i>R</i> ₁	0.0368	0.0725	0.0469
<i>wR</i> ₂	0.1268	0.2380	0.0843

Table 8

Crystallographic data for complexes [PPh₄]₂[Cu₄Pd₂[Ru₆C(CO)₁₆]₂Cl₂] (**7**), [PPh₄]₂[Pt₂[Ru₆C(CO)₁₅]₂] (**8**) and [PPh₄]₂[Cu₇[Ru₆C(CO)₁₅]₂Cl₃] (**10**)

Compound	7	8	10
Formula	C ₈₂ H ₄₀ Cl ₂ Cu ₄ O ₃₂ P ₂ Pd ₂ Ru ₁₂	C ₈₀ H ₄₀ O ₃₀ P ₂ Ru ₁₂ Pt ₂	C ₈₀ H ₄₀ Cl ₃ O ₃₀ P ₂ Ru ₁₂ Cu ₇ · C ₃ H ₆ O
Formula weight	3349.89	3146.1	3365.23
Crystal system	Triclinic	Triclinic	Triclinic
Space group	P $\bar{1}$	P $\bar{1}$	P $\bar{1}$
<i>a</i> (Å)	14.180(3)	13.9357(13)	15.8575(16)
<i>b</i> (Å)	14.877(2)	14.4853(13)	22.8021(11)
<i>c</i> (Å)	13.001(2)	13.5649(13)	15.4194(11)
α (°)	113.970(11)	114.418(2)	98.293(1)
β (°)	107.243(14)	91.999(2)	116.2860(10)
γ (°)	96.723(14)	63.146(2)	91.224(2)
<i>V</i> (Å ³)	2303.0(7)	2185.2(4)	4923.7(7)
<i>Z</i>	1	1	2
Crystal size (mm)	0.25 × 0.20 × 0.09	0.29 × 0.24 × 0.13	0.30 × 0.19 × 0.08
<i>D</i> _{calc} (g cm ⁻³)	2.413	2.391	2.270
μ (cm ⁻¹)	33.55	52.97	34.45
Full-matrix least-square	<i>F</i> ²	<i>F</i> ²	<i>F</i> ²
Reflections collected	10947	26833	58420
Unique reflections	10520	11535	26167
Reflections observed [<i>I</i> > 2 σ (<i>I</i>)]	5898	10155	18841
<i>R</i> ₁	0.0581	0.0372	0.0368
<i>wR</i> ₂	0.1732	0.0818	0.0723

became dark red in color. The solvent was evaporated under reduced pressure and the residual dark-red solid was chromatographed on SiO₂ (deactivated with 10 wt% H₂O). Two bands separated. The first red band which eluted with hexane gave, after evaporation of the solvent and recrystallization from CH₂Cl₂–hexane, red crystals of [PPh][RhRu₅C(CO)₁₆] (59 mg, 0.042 mmol, 36%) [38]. The second band eluted with CH₂Cl₂/THF (9/1). Crystallization from acetone–MeOH gave black crystals of **10** (48 mg, 0.014 mmol, 24%). IR ν (CO) 2056(m), 2026(s)

cm⁻¹. Anal. Calc. for C₈₀H₄₀Cl₃Cu₇O₃₀P₂Ru₁₂: C, 29.05; H, 1.22, N, 0.00. Found: C, 29.32; H, 1.34. N, 0.00%.

5. Supplementary material

CCDC 635296, 635297, 635294, 635295, 635192 and 635298 contain the supplementary crystallographic data for **2**, **4**, **5**, **7**, **8** and **10**. These data can be obtained free of charge via <http://www.ccdc.cam.ac.uk/conts/retrieving.html>, or from the Cambridge Crystallographic Data

Centre, 12 Union Road, Cambridge CB2 1EZ, UK; fax: (+44) 1223-336-033; or e-mail: deposit@ccdc.cam.ac.uk.

Acknowledgements

T.N. is indebted by the Grand-in-Aid for Young Scientist (B) (No. 18750053) from the Ministry of Education, Culture, Sports, and Science.

References

- [1] D.A. Roberts, G.L. Geoffroy, in: G. Wilkinson, G. Stone, E.W. Abel (Eds.), *Comprehensive Organometallic Chemistry*, vol. 6, Pergamon Press, Oxford, 1982, p. 763.
- [2] G. Wilkinson, G. Stone, E.W. Abel (Eds.), *Comprehensive Organometallic Chemistry II*, vol. 10, Pergamon Press, Oxford, 1995.
- [3] P.R. Raithby, *Platinum Metals Rev.* 42 (1998) 146.
- [4] M.A. Beswick, J. Lewis, P.R. Raithby, M.C.R. Arellano, *Angew. Chem., Int. Ed. Engl.* 36 (1997) 2227.
- [5] M.A. Beswick, J. Lewis, P.R. Raithby, M.C.R. Arellano, *Angew. Chem., Int. Ed. Engl.* 36 (1997) 291.
- [6] M.A. Beswick, J. Lewis, P.R. Raithby, M.C.R. Arellano, *J. Chem. Soc., Dalton Trans.* (1996) 4033.
- [7] S.M. Draper, A.D. Hattersley, C.E. Housecroft, A.L. Rheingold, *J. Chem. Soc., Chem. Commun.* (1992) 1365.
- [8] M.F. Hallam, D.M.P. Mingos, T. Adatia, M. McPartlin, *J. Chem. Soc., Dalton Trans.* (1988) 335.
- [9] D.S. Shephard, T. Maschmeyer, B.F.G. Johnson, J.M. Thomas, G. Sankar, D. Ozkaya, W. Zhou, R.D. Oldroyd, R.G. Bell, *Angew. Chem., Int. Ed. Engl.* 36 (1997) 2242.
- [10] A. Albinati, K.-H. Dahmen, A. Togni, L.M. Venanzi, *Angew. Chem., Int. Ed. Engl.* 24 (1985) 766.
- [11] M. Fajardo, M.P. Gómez-sal, H.D. Holden, B.F.G. Johnson, J. Lewis, R.C.S. McQueen, P.R. Raithby, *J. Organomet. Chem.* 267 (1984) C25.
- [12] B.T. Heaton, L. Strona, S. Martinengo, D. Strumolo, V.G. Albano, D. Braga, *J. Chem. Soc., Dalton Trans.* (1983) 2175.
- [13] A.J.W. Johnson, B. Spencer, L.F. Dahl, *Inorg. Chim. Acta* 227 (1997) 269.
- [14] R.C.B. Copley, C.M. Hill, D.M.P. Mingos, *J. Clust. Sci.* 6 (1997) 71.
- [15] C.E. Housecroft, A.L. Rheingold, M.S. Shongwe, *J. Chem. Soc., Chem. Commun.* (1988) 1630.
- [16] S.R. Drake, K. Henrick, B.F.G. Johnson, J. Lewis, M. McPartlin, J. Morris, *J. Chem. Soc., Chem. Commun.* (1986) 928.
- [17] B.F.G. Johnson, D.A. Kaner, J. Lewis, P.R. Raithby, *J. Chem. Soc., Chem. Commun.* (1981) 753.
- [18] R. Reina, O. Riba, O. Rossell, M. Seco, P. Gómez-sal, A. Martín, D. Montauzon, A. Mari, *Organometallics* 17 (1998) 4127.
- [19] L.H. Gade, B.F.G. Johnson, J. Lewis, M. McPartlin, H.R. Powell, *J. Chem. Soc., Dalton Trans.* (1992) 921.
- [20] B.F.G. Johnson, W.-L. Kwik, J. Lewis, P.R. Raithby, V.P. Saharan, *J. Chem. Soc., Dalton Trans.* (1991) 1037.
- [21] L.H. Gade, B.F.G. Johnson, J. Lewis, M. McPartlin, H.R. Powell, *J. Chem. Soc., Chem. Commun.* (1990) 110.
- [22] L.J. Farrugia, *J. Chem. Soc., Chem. Commun.* (1987) 147.
- [23] P. Braunstein, J. Rose, A. Tiripicchio, M.T. Camellini, *Angew. Chem., Int. Ed. Engl.* 24 (1985) 767.
- [24] M.P. Gómez-sal, B.F.G. Johnson, J. Lewis, P.R. Raithby, S.N.A.B. Syed-Mustaffa, *J. Organomet. Chem.* 272 (1984) C21.
- [25] S. Ermer, K. King, K.I. Hardcastle, E. Rosenberg, A.M.M. Lanfredi, A. Tiripicchio, M.T. Camellini, *Inorg. Chem.* 22 (1983) 1339.
- [26] R.D. Adams, B. Captain, *J. Organomet. Chem.* 689 (2004) 4521.
- [27] B.F.G. Johnson, S. Hermans, T. Khimiyak, *Eur. J. Inorg. Chem.* (2003) 1325.
- [28] K.-F. Yung, W.-T. Wong, *Angew. Chem., Int. Ed.* 42 (2003) 553.
- [29] T. Nakajima, A. Ishiguro, Y. Wakatsuki, *Angew. Chem., Int. Ed.* 39 (2000) 1131.
- [30] E.G. Mednikov, C.G. Fry, L.F. Dahl, *Angew. Chem., Int. Ed.* 44 (2005) 786.
- [31] A.B. Antonova, A.A. Johansson, N.A. Deykhina, D.A. Pogrebnyakov, N.I. Pavlenko, A.I. Rubaylo, F.M. Dolgushin, P.V. Petrovskii, A.G. Ginzburg, *J. Organomet. Chem.* 577 (1999) 238.
- [32] B.K. Teo, H. Zhang, *J. Clust. Sci.* 12 (2001) 349.
- [33] N.T. Tran, M. Kawano, D.R. Powell, R.K. Hayashi, C.F. Campana, L.F. Dahl, *J. Am. Chem. Soc.* 121 (1999) 5945.
- [34] B.K. Teo, H. Zhang, X. Shi, *J. Am. Chem. Soc.* 115 (1993) 8489.
- [35] T. Chihara, M. Sato, H. Konomoto, S. Kamiguchi, H. Ogawa, Y. Wakatsuki, *J. Chem. Soc., Dalton Trans.* (2000) 2295.
- [36] T. Nakajima, A. Ishiguro, Y. Wakatsuki, *Angew. Chem., Int. Ed.* 40 (2001) 1066.
- [37] T. Adatia, H. Curtis, B.F.G. Johnson, J. Lewis, M. McPartin, J. Morris, *J. Chem. Soc., Dalton Trans.* (1994) 3069.
- [38] T. Nakajima, H. Konomoto, H. Ogawa, Y. Wakatsuki, *J. Organomet. Chem.* (2007), doi:10.1016/j.jorganchem.2007.07.005.
- [39] J.N. Nicholls, M.D. Vargas, J. Hriljac, M. Sailor, *Inorg. Synth.* 26 (1989) 283.
- [40] C.-M.T. Hayward, J.R. Shapely, *Inorg. Chem.* 21 (1982) 3816.
- [41] H.M. Colquhoun, S.M. Doughty, J.F. Stoddart, A.M.Z. Slawin, D.J. Williams, *J. Chem. Soc., Dalton Trans.* (1986) 1639.
- [42] T. Ukai, H. Kawazura, Y. Ishii, *J. Organomet. Chem.* 65 (1974) 253.
- [43] K. Moseley, P.M. Maitlis, *J. Chem. Soc., Dalton Trans.* (1974) 169.
- [44] J.A. McCleverty, G. Wilkinson, *Inorg. Synth.* 8 (1966) 211.